SAR ABSOLUTE RANGING – VALIDATION AND APPLICATION OF SAR GEODESY PROCESSOR USING ECMWF REANALYSIS AND OPERATIONAL DATA

Xiaoying Cong[(1)], Ulrich Balss[(2)], Steffen Suchandt[(2)], Michael Eineder[(2)], Hartmut Runge[(2)]

(1) Chair of Remote Sensing Technology (LMF), Technische Universität München (TUM),
(2) Remote Sensing Technology Institute (IMF), German Aerospace Center (DLR)

ABSTRACT

Range accuracy of synthetic aperture radar using modern satellites has been proven in centimeter-range after consideration of geodynamic, atmospheric effects and systematic errors; it is so-called Imaging Geodesy technique. Based on this technique, we have proposed the next-generation of Synthetic Aperture Radar (SAR) products and developed operational software SAR Geodesy Processor in the previous paper. In this paper, we are concentrated on validation of processor and accuracy analysis on a global-scale. Two datasets with different spatial resolutions generated from European Centre for Medium-Range Weather Forecast are used to compensate atmospheric refraction effect in range. At the end, we apply corrections on a Sentinel interferogram by using both datasets.

Index Terms— SAR, absolute ranging, atmospheric refraction, SAR Geodesy Processor, ECMWF

1. INTRODUCTION

The range accuracy of Synthetic Aperture Radar (SAR) is affected mainly by four factors: systematic errors, satellite orbit errors, atmospheric propagation delay and geodynamic effects [1, 2]. Considering the influence of the error sources on range, the measured range *R*' is different from the expected range *R* and may be written as:

$$R' = R + R_{sys} + R_{orb} + R_{geod} + R_{atmo} \qquad (1)$$

where R_{sys}, R_{orb}, R_{atmo}, R_{geod} are range errors caused by systematic errors, satellite orbit error, atmospheric delay and geodetic effects, respectively. Orbit accuracy of modern SAR satellite has been improved to around centimeter-level and stable in time [3], which ensures the centimeter-range accuracy of range measurements after consideration of corrections. Among all three groups of influences, atmospheric effects, more detailed, tropospheric delay plays an inevitable role and affects overall accuracy of absolute ranging method. Different from geodynamic effects and systematic errors, which could be well-modeled or calibrated with experiments, tropospheric delay varies both in time and location. In order to achieve the centimeter-range accuracy in range direction, direct integration method was developed based four-dimensional Numerical Weather Prediction (NWP) datasets [4, 5].

In our previous paper [6], we have introduced operational software based on Imaging Geodesy technique and further developments [4-7]. In this paper, we are concentrated on validation of processor, and will perform accuracy analysis on a global scale. Two datasets from European Centre for Medium-Range Weather Forecast (ECMWF) are prepared and used to compensate the tropospheric delay. Reanalysis dataset, ERA-Interim, has been mainly used for the validation. Operational data, which has a limited access, has a better spatial resolution and is for the first time used for accuracy assessment and interferometric application.

2. SGP FRAMWORK

We have developed the SAR geodesy processor SGP, a software system that integrates several kinds of corrections for propagation path delays as well as for geodetic effects. Its main purpose is to automatically retrieve and to annotate the aforementioned corrections for standard SAR image products or arbitrary point clouds extracted from such data. While designing the SGP, emphasis was put on easy extensibility to new input products and sensors on one side and on flexible interfaces for the necessary auxiliary data, such as numerical weather prediction (NWP), total electron content (TEC) or solid earth tides (SET) on the other.

One essential part of the SGP, whose flow chart is shown in Fig. x, is the definition of a set of coordinates with regular or irregular spacing, referred to as the grid. The grid structure and coordinate projection correspond to the ones of the input data product. By using just the input product's meta-information, i.e. without the necessity of reading actual image data, the SGP retrieves auxiliary data from local databases by a spatio-temporal search and interpolation and uses them to calculate corrections for ionospheric and tropospheric path delays as well as for offsets due to SET. All corrections, single and total ones, are assigned respectively to each grid point. Augmented with

this information, the grid points are then formatted to obtain an output correction data product.

3. ACCURACY ASSESSMENT BASED ON ECMWF REANALYSIS DATA

In this section, ERA-Interim data from ECMWF [8] is used to estimate tropospheric delay based on direct integration method [5,6]. For a global analysis, Zenith Path Delay (ZPD) on permanent stations of International GNSS Service has been used as reference [9] and compared with integrated ZPD using ERA-Interim data in section 3.1. In section 3.2, Slant Path Delay (SPD) estimated from SAR range measurements are used to validate the integrated SPD.

3.1 Global accuracy assessment based on GPS ZPD

For global validation, 220 permanent GPS stations have been selected from IGS. For each analysis time of ERA-Interim product from 1.Jan.2014 until 31.Dec.2014, a reference GPS ZPD was selected or interpolated. Residues are calculated between integrated ZPD using ERA-Interim and reference GPS ZPD. Mean value of residues over entire duration is calculated for each station and presented in Figure 1. The maximum is about 22.7 mm and the minimum is around -13.6 mm. About 90% of stations have a bias less than 10.0 mm, and 50% of stations have a bias less than 5.0 mm.

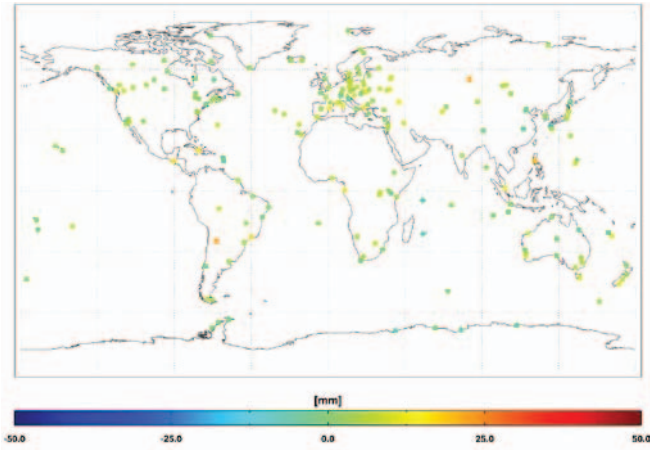

Figure 1. Mean value of residues between GPS ZPD and integrated ZPD using ERA-Interim over entire 2014.

Standard deviation of residues over entire duration is calculated for each station and presented in Figure 2. The maximum is about 26.2 mm and the minimum is around 12.8 mm. The variation of standard deviation presents a clear correlation with latitude, since the water vapor content is highly correlated with latitude.

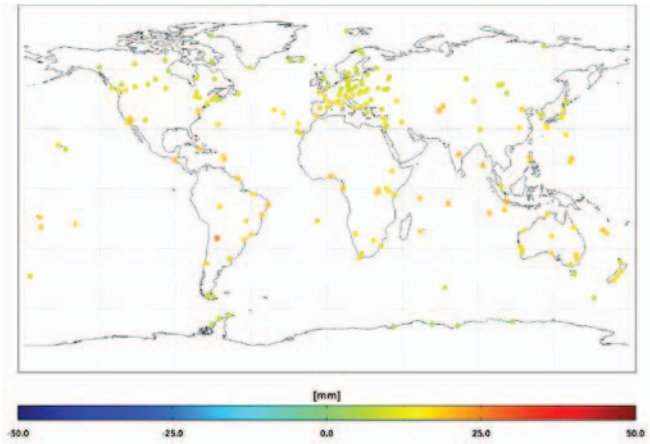

Figure 2. Standard deviation of residues between GPS ZPD and integrated ZPD using ERA-Interim over entire 2014.

3.2 Validation of SPD Based on Corner Reflector Experiments

In [5, 7], slant range measurements between corner reflector and SAR satellite can be used an independent measurement for atmospheric delay after correcting geodynamic effects, systematic errors and ionospheric delay. Corner reflector (CR) experiments presented in [7] have been used for validation. In Figure 3, the scatter plot of estimated SAR SPD and integrated SPD using ERA-Interim is plotted. Three clusters of points in blue, red and green indicate three incidence angles: ~30°, ~40° and ~50°. The residues are calculated between two SPDs have been calculated. Excluding the outlier (red cluster), the standard deviation of residues is around 2.0 cm for three clusters.

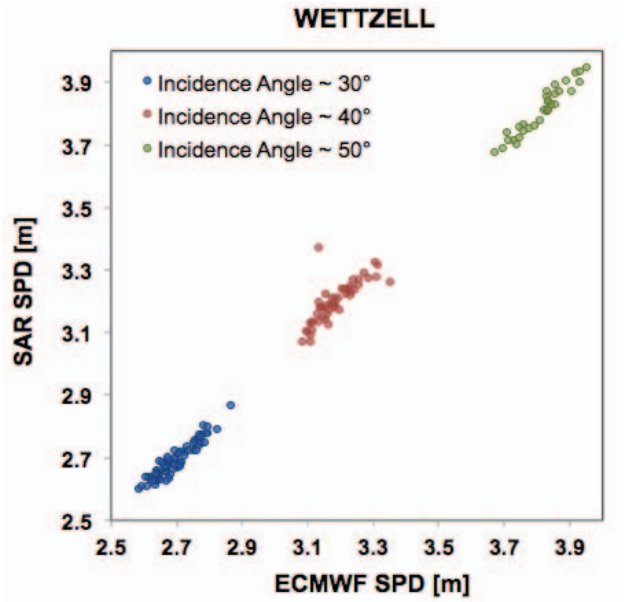

Figure 3. Scatter plot of estimated SAR SPD and integrated SPD using ERA-Interim is plotted. Three clusters of points in blue, red and green indicate three incidence angles: ~30°, ~40° and ~50°.

4. ACCURACY COMPARISON BETWEEN OPERATIONAL AND REANALYSIS DATA

Operational data, unlike ERA-Interim, is produced with up-to-date assimilation version and has a varied resolution for the whole period. From 2013, operational data increased the vertical level from 91 to 137 (up to 0.01 hPa). The horizontal resolution is about 16 km, comparing to 80 km of ERA-Interim data. We collected three months operational data from 1.Jan. 2015 to 31.Mar.2015 from Wettzell test site [5-7].

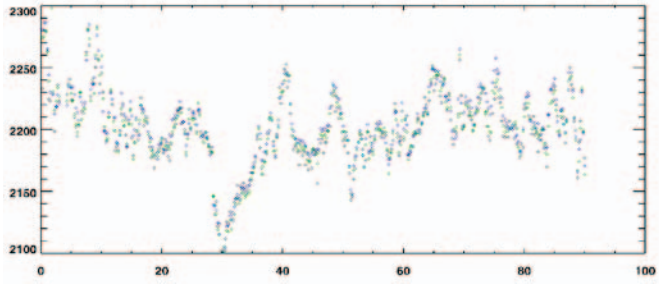

Figure 4. Integrated ZPDs using ERA-Interim (blue circle) and operational data (green circle)

For comparison, two ZPDs have been integrated using both ERA-Interim and operational data and presented in Figure 4. Similar to validation in section 3.1, GPS ZPDs on Wettzell test site are used as reference. The residues are calculated based on reference GPS ZPDs. The mean value of residues is about 1.1 mm by using operational data, where the mean value is about 4.4 mm by using ERA-Interim data. The standard deviation is 6.6 mm with operational data, which is about 1.5 mm better than using reanalysis data.

5. INTERFEROMETRIC APPLICATIONS

For interferometric application, two SAR images acquired from SENTINEL-1A with Interferometric Wide (IW) Swath mode are selected. The master image was acquired on 2.Jan.2015 and the slave image on 21.Dec.2015 5:33UTC. The center latitude is about 49.65° and the center longitude is about 9.22°. Both reanalysis and operational data are used to calculate tropospheric delay. Corrections with different NWP inputs are generated with SGP. Original phase, as well as tropospheric phases and compensated phases are shown in Figure 5. Obviously, the tropospheric phase estimated with operational data has better correlation with original interferometric phase.

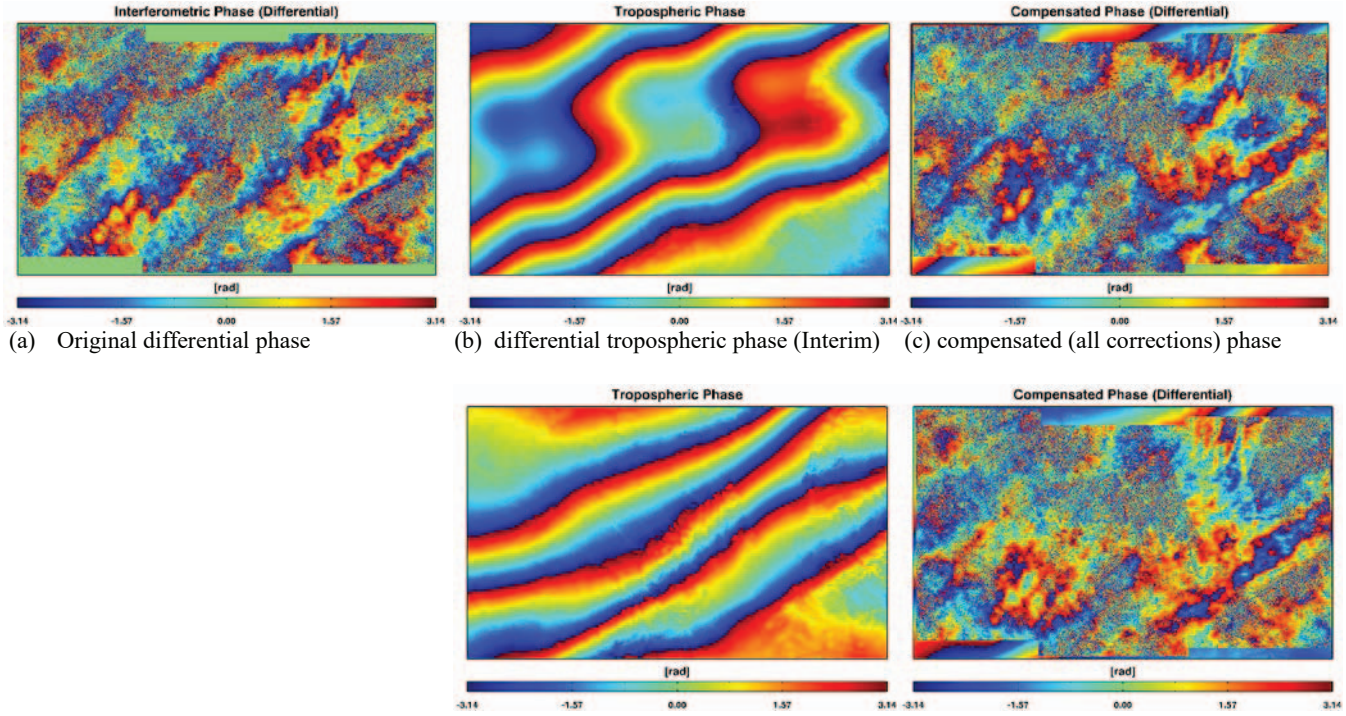

(a) Original differential phase (b) differential tropospheric phase (Interim) (c) compensated (all corrections) phase

(d) differential tropospheric phase (operational) (e) compensated (all corrections) phase

Figure 5. Interferometric application with a SENTINEL interferogram. Corrections with both ERA-Interim and operational data are generated with SGP.

6. SUMMARY AND OUTLOOK

In this paper, ERA-Interim data is validated globally with respect to GPS references. The standard deviation of residues in 2014 varies from about 12.8 to 22.6 mm. This accuracy is highly dependent on the latitude, or more detailed, on the distribution of water vapor. Based on the comparison in Wettzell, operational data is about 1.5 mm more accurate than ERA-Interim. For interferometric applications, the tropospheric phase generated by operational data is clearly correlated with pattern in original interferometric phase, whereas ERA-Interim misinterpreted the tropospheric variation.

7. ACKNOWLEDGMENT

Remote Sensing Technology Institute (DLR-IMF) has applied access to ECMWF meteorological archive, which was approved by Deutscher Wetterdienst.

8. REFERENCE

[1] M. Eineder, C. Minet, P. Steigenberger, X.Y. Cong, and T. Fritz, "Imaging Geodesy – toward Centimeter-Level Ranging Accuracy with TerraSAR-X," *IEEE Trans. Geosc. Remote Sens.,* vol. 49, pp. 661-671, 2011.

[2] A. Schubert, M. Jehle, D. Small, and E. Meier, "Mitigation of Atmospheric Pertubations and Solid Earth Movements in a TerraSAR-X Time-Series," Journal of Geodesy, vol. 86, pp. 257-270, 2011.

[3] Yoon Y T, Eineder M, Yague-Martinez N, et al. TerraSAR-X precise trajectory estimation and quality assessment[J]. IEEE Transactions on Geoscience and Remote Sensing, vol. 47(6), pp.: 1859-1868, 2009.

[4] M. Eineder, U. Balss, S. Suchandt, C. Gisinger, X.Y. Cong, and H. Runge, "A Definition of Next-Generation SAR Products for Geodetic Applications," *Proc. IGARSS 2015,* Milan, Italy, pp. 1638-1641, 2015.

[5] Cong, X., Balss, U., Eineder, M., Fritz, T., Imaging Geodesy – Centimeter-Level Ranging Accuracy With TerraSAR-X: An Update. IEEE Geoscience and Remote Sensing Letters 9, pp. 948-952, 2012.

[6] Cong, X., SAR Interferometry for Volcano Monitoring: 3D-PSI Analysis and Mitigation of Atmospheric Refractivity. Dissertation, Technische Universität München, 2014.

[7] U. Balss, C. Gisinger, X.Y. Cong, R. Brcic, S. Hackel, and M. Eineder, "Precise Measurements of the Absolute Localization Accuracy of TerrSAR-X on the Base of Far-Distributed Test Sites," *Proc. EUSAR 2014,* Berlin, Germany, pp. 993-996, 2014.

[8] Dee, D. P., Uppala, S. M., Simmons, A. J., Berrisford, P., Poli, P., Kobayashi, S., Andrae, U., Balmaseda, M. A., Balsamo, G., Bauer, P., Bechtold, P., Beljaars, A. C. M., van de Berg, L., Bidlot, J., Bormann, N., Delsol, C., Dragani, R., Fuentes, M., Geer, A. J., Haimberger, L., Healy, S. B., Hersbach, H., Hólm, E. V., Isaksen, L., Kållberg, P., Köhler, M., Matricardi, M., McNally, A. P., Monge-Sanz, B. M., Morcrette, J.-J., Park, B.-K., Peubey, C., de Rosnay, P., Tavolato, C., Thépaut, J.-N. and Vitart, F., The ERA-Interim reanalysis: configuration and performance of the data assimilation system. Q.J.R. Meteorol. Soc., 137: 553–597, 2011.

[9] Dow, J.M., Neilan, R. E., and Rizos, C., The International GNSS Service in a changing landscape of Global Navigation Satellite Systems, Journal of Geodesy vol. 83, pp: 191–198, 2009.